

## Supporting Material

### Observational data

#### Atmospheric temperature data

Satellite-based estimates of the temperature of the lower troposphere (TLT) were provided by two different groups: 1) Remote Sensing Systems in Santa Rosa, California (RSS) [Mears et al., 2007], and 2) the University of Alabama at Huntsville (UAH) [Christy et al., 2007]. Note that a third group, the Center for Satellite Applications and Research, NOAA/National Environmental Satellite, Data, and Information Service, Camp Springs, Maryland (STAR) [Zou et al., 2006], currently provides satellite-based estimates of atmospheric temperature change for the lower stratosphere and mid- to upper troposphere only.

All analyses reported on here rely on the following versions of these temperature datasets:

1. Version 3.2 of RSS TLT data, downloaded from <http://www.remss.com/data/msu/data/netcdf> on 1/7/2011;
2. Version 3.3 of RSS TLT data, downloaded from <http://www.remss.com/data/msu/data/netcdf> on 2/7/2011;

3. Version 5.3 of UAH TLT data, downloaded from <http://vortwx.nsstc.uah.edu/data/msu/t2lt> on 1/7/2011.

All RSS and UAH TLT datasets were in the form of monthly means on  $2.5^\circ \times 2.5^\circ$  latitude/longitude grids, and span the 384-month analysis period considered here (January 1979 to December 2010). We analyzed complete years only; data available for the last several months of 1978 and the initial months of 2011 were not used. The UAH TLT data have global coverage, while RSS TLT datasets extend from  $82.5^\circ\text{N}$  to  $70^\circ\text{S}$ .

There are two reasons why the RSS TLT coverage is restricted to  $82.5^\circ\text{N}$ - $70^\circ\text{S}$ :

1. Poleward of  $82.5^\circ$ , there are virtually no MSU brightness temperature measurements from the central view angle of the satellite “swath”;
2. In the Southern Hemisphere, the reliable estimation of brightness temperatures is hampered by the large (and poorly-known) surface emissivity contribution from snow- and ice-covered areas of the Antarctic continent which lie above 3,000 meters [*Swanson, 2003*].

To exclude any impact of spatial coverage differences on trend comparisons, we calculated all spatial averages of observed and simulated TLT changes over the area of common coverage in the RSS and UAH TLT data ( $82.5^\circ\text{N}$ - $70^\circ\text{S}$ ).

## Sea surface temperature data

In Figure 7B, we used data from version 3b of the NOAA Extended Reconstructed Sea Surface Temperature dataset (ERSST) [*Smith et al.*, 2008] for calculating spatially-averaged SST changes over the Niño 3.4 region (5°N-5°S; 170°W-120°W). ERSST data were available from January 1854 to December 2010 in the form of monthly means on a regular 2° × 2° latitude/longitude grid. Reconstruction of high-frequency SST anomalies involved use of empirically-derived spatial modes of variability to interpolate observations in times of sparse coverage. Further details of the ERSST dataset are available online at <http://www.ncdc.noaa.gov/oa/climate/research/sst/ersstv3.php>.

## Details of model output

We used model output from phase 3 of the Coupled Model Intercomparison Project (CMIP-3) [*Meehl et al.*, 2007; *IPCC*, 2007]. CMIP-3 was an important scientific resource for the Fourth Assessment Report of the Intergovernmental Panel on Climate Change (IPCC AR4). As noted in the main text, we analyzed three different types of simulation in the CMIP-3 multi-model archive:

1. Pre-industrial control runs with no changes in external influences on climate, which provide information on internal climate noise;

2. 20th century (20CEN) runs with estimated historical changes in human and (in some cases) natural external forcings (see Table S1); and
3. Simulations with 21st century changes in greenhouse gases and anthropogenic aerosols prescribed according to the SRES A1B scenario [*Nakicenovic and Swart, 2000*].

SRES stands for the IPCC Special Report on Emissions Scenarios. Assumptions underlying the A1B scenario relate to such factors as population growth, economic development, rate of introduction of new technologies, and the mix of fossil-fuel intensive and non-fossil fuel energy sources [*IPCC, 2007; Nakicenovic and Swart, 2000*]. The computed radiative forcing in 2100 in the SRES A1B scenario corresponds to an “approximate carbon dioxide equivalent concentration” of 850 ppm [*IPCC, 2007*].

Climate output from these and other simulations were supplied to the scientific community through the U.S. Department of Energy’s Program for Climate Model Diagnosis and Intercomparison (PCMDI). Documentation on the models and simulations used here is available at [http://www-pcmdi.llnl.gov/ipcc/model\\_documentation/ipcc\\_model\\_documentation.php](http://www-pcmdi.llnl.gov/ipcc/model_documentation/ipcc_model_documentation.php). As described in Tables S2 and S3, this documentation provided sufficient information to permit calculation of synthetic TLT from the CMIP-3 control, 20CEN, and A1B runs. Splicing of synthetic TLT data from the 20CEN and A1B runs was facilitated by documentation on the spawning dates of A1B runs, available at: [http://www-pcmdi.llnl.gov/ipcc/info\\_for\\_analysts.php#time\\_info](http://www-pcmdi.llnl.gov/ipcc/info_for_analysts.php#time_info).

Official designations of the modeling groups that provided simulation output analyzed here are listed below (with model acronyms in brackets):

1. Bjerknes Center for Climate Research, Norway [BCCR-BCM2.0].
2. Canadian Centre for Climate Modelling and Analysis, Canada [CCCma-CGCM3.1(T47) and CCCma-CGCM3.1(T63)].
3. National Center for Atmospheric Research, U.S.A. [CCSM3 and PCM].
4. Météo-France/Centre National de Recherches Météorologiques, France [CNRM-CM3].
5. Commonwealth Scientific and Industrial Research Organization (CSIRO) Atmospheric Research, Australia [CSIRO-Mk3.5].
6. Max-Planck Institute for Meteorology, Germany [ECHAM5/MPI-OM].
7. Institute for Atmospheric Physics, China [FGOALS-g1.0].
8. Geophysical Fluid Dynamics Laboratory, U.S.A. [GFDL-CM2.0 and GFDL-CM2.1].
9. Goddard Institute for Space Studies, U.S.A. [GISS-AOM, GISS-EH, and GISS-ER].
10. Istituto Nazionale di Geofisica e Vulcanologia [INGV-SXG].
11. Institute for Numerical Mathematics, Russia [INM-CM3.0].
12. Institute Pierre Simon Laplace, France [IPSL-CM4].

13. Center for Climate System Research, National Institute for Environmental Studies, and Frontier Research Center for Global Change, Japan [MIROC3.2(medres) and MIROC3.2(hires)].
14. Meteorological Research Institute, Japan [MRI-CGCM2.3.2].
15. Hadley Centre for Climate Prediction and Research, U.K. [UKMO-HadCM3 and UKMO-HadGEM1].

## Forcings used in 20CEN runs

Details of the natural and anthropogenic forcings used by modeling groups in their IPCC 20CEN simulations are given in Table S1. This Table was compiled using information that participating modeling centers provided to PCMDI (see [http://www-pcmdi.llnl.gov/ipcc/model\\_documentation/ipcc\\_model\\_documentation.php](http://www-pcmdi.llnl.gov/ipcc/model_documentation/ipcc_model_documentation.php)), and with additional information obtained in response to specific inquiries. All model acronyms used in the Table are defined in the previous Section.

A total of 11 different forcings are listed in Table S1. A letter ‘Y’ denotes inclusion of a specific forcing. As used here, ‘inclusion’ signifies the specification of time-varying forcings, with changes on interannual and longer timescales. Forcings that were varied over the seasonal cycle only, or not at all, are identified with a dash. A question mark indicates a case where there is uncertainty regarding inclusion of the forcing.

Results in Table S1 are stratified by inclusion or omission of volcanic forcing (V or No-V, respectively). Nine of the 10 V models explicitly incorporated volcanic aerosols. One V model (MRI-CGCM2.3.2) represented volcanic effects in a more indirect manner, using estimated volcanic forcing data from *Sato et al.* [1993] to adjust the solar irradiance at the top of the model atmosphere. There is some ambiguity regarding the treatment of volcanic aerosol effects in the 20CEN run of the INM-CM3.0 model. It is likely that the INM group, like MRI, also used some form of albedo or solar irradiance adjustment to represent volcanic aerosol effects on climate.

The HadGEM1 model incorporated solar and volcanic forcing only in run2 of its 20CEN simulation – run1 (from which the sole realization of the SRES A1B simulation was spawned) included anthropogenic forcings only.

Note that the V versus No-V partitioning also separates models with ‘total’ external forcing (natural plus anthropogenic) from models with primarily anthropogenic forcing.

While all modeling groups used very similar changes in well-mixed greenhouse gases, the changes in other forcings were not prescribed as part of the experimental design. In practice, each group employed different combinations of 20th century forcings, and often used different datasets for specifying individual forcings. The start and end dates for the 20CEN experiment varied among groups (see Table S2).

## Supporting Material References

Christy, J. R., W. B. Norris, R. W. Spencer, and J. J. Hnilo (2007), Tropospheric temperature change since 1979 from tropical radiosonde and satellite measurements, *J. Geophys. Res.*, *112*, D06102, doi:10.1029/2005JD006881

IPCC (Intergovernmental Panel on Climate Change) (2007), Summary for Policymakers, in *Climate Change 2007: The Physical Science Basis. Contribution of Working Group I to the Fourth Assessment Report of the Intergovernmental Panel on Climate Change*, edited by S. Solomon, D. Qin, M. Manning, Z. Chen, M. Marquis, K. B. Averyt, M. Tignor, and H. L. Miller HL, Cambridge University Press, Cambridge, United Kingdom and New York, N. Y., U. S. A.

Mears, C. A., F. J. Wentz, B. D. Santer, K. E. Taylor, and M. F. Wehner (2007), Relationship between temperature and precipitable water changes over tropical oceans, *Geophys. Res. Lett.*, *34*, L24709, doi:10.1029/2007GL031936.

Meehl, G. A., et al. (2007), The WCRP CMIP3 multi-model dataset: A new era in climate change research, *Bull. Amer. Meteor. Soc.*, *88*, 1383-1394.

Nakicenovic, N., and R. Swart R (Eds.) (2000), *Special Report on Emissions Scenarios. A Special Report of Working Group III of the Intergovernmental Panel on Climate Change*, Cambridge University Press, Cambridge, U. K.



Press, W. H., S. A. Teukolsky, W. T. Vetterling, and B. P. Flannery (1992), *Numerical Recipes in FORTRAN: The Art of Scientific Computing*, Cambridge University Press, New York, 963 pp.

Sato, M., J. E. Hansen, M. P. McCormick, and J. B. Pollack (1993), Stratospheric aerosol optical depths, 1850-1990, *J. Geophys. Res.*, *98*, 22987-22994.

Smith, T. M., R. W. Reynolds, T. C. Peterson, and J. Lawrimore (2008), Improvements to NOAA's historical merged land-ocean surface temperature analysis (1880-2006), *J. Clim.*, *21*, 2283-2296.

Swanson, R. E. (2003), Evidence of possible sea-ice influence on Microwave Sounding Unit tropospheric temperature trends in polar regions, *Geophys. Res. Lett.*, *30*, 2040, doi:10.1029/2003GL017938.

Zou, C.-Z., et al. (2006), Recalibration of Microwave Sounding Unit for climate studies using simultaneous nadir overpasses, *J. Geophys. Res.*, *111*, D19114, doi:10.1029/2005JD006798.

## Captions for Tables in Supporting Text

**Table S1:** Forcings used in CMIP-3 20CEN simulations. Results are partitioned into V and No-V models (first 11 and last 9 rows, respectively). A letter ‘Y’ denotes inclusion of a specific forcing. A question mark indicates a case where there is uncertainty regarding inclusion of the forcing. Note that the V versus No-V partitioning also captures other important forcing differences between these two groups of models.

**Table S2:** Basic information relating to the splicing of the CMIP-3 20CEN/A1B runs. Information is provided for the number of 20CEN/A1B realizations, the start and end years of the spliced runs, the length of the spliced runs (in months), the end year of the 20CEN runs, and the initial year of the A1B run. More detailed information regarding the processing of the 20CEN and A1B runs is appended at the end of the Table.

**Table S3:** Basic information relating to the CMIP-3 pre-industrial control integrations. Information is provided for the number of control run realizations, the control run start and end years, and the control run length (in months). The start date of each control run is arbitrary. More detailed information regarding the processing of the control run output is appended at the end of the Table.

Table S1: Forcings used in IPCC simulations of 20th century climate change.

Model	G	O	SD	SI	BC	OC	MD	SS	LU	SO	VL
1 CCSM3	Y	Y	Y	-	Y	Y	-	-	-	Y	Y
2 GFDL-CM2.0	Y	Y	Y	-	Y	Y	-	-	Y	Y	Y
3 GFDL-CM2.1	Y	Y	Y	-	Y	Y	-	-	Y	Y	Y
4 GISS-EH	Y	Y	Y	Y	Y	Y	Y	Y	Y	Y	Y
5 GISS-ER	Y	Y	Y	Y	Y	Y	Y	Y	Y	Y	Y
6 INM-CM3.0	Y	-	Y	-	-	-	-	-	-	Y	?
7 MIROC3.2(medres)	Y	Y	Y	Y	Y	Y	Y	Y	Y	Y	Y
8 MIROC3.2(hires)	Y	Y	Y	Y	Y	Y	Y	Y	Y	Y	Y
9 MRI-CGCM2.3.2	Y	-	Y	-	-	-	-	-	-	Y	Y
10 UKMO-HadCM3	Y	Y	Y	Y	-	-	-	-	-	Y	Y
1 BCCR-BCM2.0	Y	-	Y	-	-	-	-	-	-	-	-
2 CCCma-CGCM3.1(T47)	Y	-	Y	-	-	-	-	-	-	-	-
3 CCCma-CGCM3.1(T63)	Y	-	Y	-	-	-	-	-	-	-	-
4 CSIRO-Mk3.5	Y	-	Y	-	?	?	?	?	?	?	-
5 ECHAM5/MPI-OM	Y	Y	Y	Y	-	-	-	-	-	-	-
6 FGOALS-g1.0	Y	-	Y	?	-	-	-	-	-	-	-
7 GISS-AOM	Y	-	Y	-	-	-	-	Y	-	-	-
8 INGV-SXG	Y	-	Y	-	-	-	-	-	-	-	-
9 PCM	Y	Y	Y	-	-	-	-	-	-	Y	Y
10 UKMO-HadGEM1	Y	Y	Y	Y	Y	Y	-	-	Y	-	-

G = Well-mixed greenhouse gases

O = Tropospheric and stratospheric ozone

SD = Sulfate aerosol direct effects

SI = Sulfate aerosol indirect effects

BC = Black carbon

OC = Organic carbon

MD = Mineral dust

SS = Sea salt

LU = Land use change

SO = Solar irradiance

VL = Volcanic aerosols.

Table S2: Basic information relating to the splicing of CMIP-3 20CEN and A1B simulations.

	Model	Realization	20CEN/A1B year 1	20CEN/A1B year $N$	$N \times 12$ (months)	20CEN year $M$	A1B year 1
1	BCCR-BCM2.0	run1	1850	2099	3000	1999	2000
2	CCCma-CGCM3.1(T47)	run1	1850	2300	5412	2000	2001
3	CCCma-CGCM3.1(T47)	run2	1850	2200	4212	2000	2001
4	CCCma-CGCM3.1(T47)	run3	1850	2200	4212	2000	2001
5	CCCma-CGCM3.1(T47)	run4	1850	2200	4212	2000	2001
6	CCCma-CGCM3.1(T47)	run5	1850	2200	4212	2000	2001
7	CCCma-CGCM3.1(T63)	run1	1850	2300	5412	2000	2001
8	CCSM3	run1	1870	2099	2760	1999	2000
9	CCSM3	run2	1870	2099	2760	1999	2000
10	CCSM3	run3	1870	2099	2760	1999	2000
11	CCSM3	run5	1870	2199	3960	1999	2000
12	CCSM3	run6	1870	2099	2760	1999	2000
13	CCSM3	run7	1870	2349	5760	1999	2000
14	CCSM3	run9	1870	2099	2760	1999	2000
15	CSIRO-Mk3.5	run1	1871	2300	5160	2000	2001
16	ECHAM5/MPI-OM	run1	1860	2200	4092	2100	2001
17	ECHAM5/MPI-OM	run2	1860	2300	5292	2050	2001
18	ECHAM5/MPI-OM	run3	1860	2200	4092	2100	2001
19	ECHAM5/MPI-OM	run4	1860	2100	2892	2000	2001
20	FGOALS-g1.0	run1	1850	2199	4200	1999	2000
21	FGOALS-g1.0	run2	1850	2199	4200	1999	2000
22	FGOALS-g1.0	run3	1850	2199	4200	1999	2000
23	GFDL-CM2.0	run1	1861	2300	5280	2000	2001
24	GFDL-CM2.1	run1	1861	2300	5280	2000	2001
25	GISS-AOM	run1	1850	2100	3012	2000	2001
26	GISS-AOM	run2	1850	2100	3012	2000	2001

Table S2: Basic information relating to the splicing of CMIP-3 20CEN and A1B simulations (continued).

Model	Realization	20CEN/A1B year 1	20CEN/A1B year $N$	$N \times 12$ (months)	20CEN year $M$	A1B year 1
27 GISS-EH	run1	1880	2099	2640	1999	2000
28 GISS-EH	run2	1880	2099	2640	1999	2000
29 GISS-EH	run3	1880	2099	2640	1999	2000
30 GISS-ER	run1	1880	2300	5052	2003	2004
31 GISS-ER	run2	1880	2200	3852	2003	2004
32 GISS-ER	run3	1880	2200	3852	2100	2004
33 GISS-ER	run4	1880	2200	3852	2003	2004
34 GISS-ER	run5	1880	2200	3852	2003	2004
35 INGV-SXG	run1	1870	2100	2772	2000	2001
36 INM-CM3.0	run1	1871	2200	3960	2000	2001
37 MIROC3.2(hires)	run1	1900	2100	2412	2000	2001
38 MIROC3.2(medres)	run1	1850	2300	5412	2000	2001
39 MIROC3.2(medres)	run2	1850	2100	3012	2000	2001
40 MIROC3.2(medres)	run3	1850	2100	3012	2000	2001
41 MRI-CGCM2.3.2	run1	1851	2100	3000	2000	2001
42 MRI-CGCM2.3.2	run2	1851	2100	3000	2000	2001
43 MRI-CGCM2.3.2	run3	1851	2100	3000	2000	2001
44 MRI-CGCM2.3.2	run4	1851	2100	3000	2000	2001
45 MRI-CGCM2.3.2	run5	1851	2100	3000	2000	2001
46 PCM	run1	1871	2098	2736	1999	2000
47 PCM	run2	1961	2299	4068	1999	2000
48 PCM	run3	1872	2199	3936	1999	2000
49 PCM	run4	1871	2099	2748	1999	2000
50 UKMO-HadCM3	run1	1947	2105	1908	1999	2000
51 UKMO-HadGEM1	run1	1860	2198	4068	1999	2000

**Table S2: Processing notes for splicing of 20CEN and A1B runs**

Documentation available at PCMDI ([http://www-pcmdi.llnl.gov/ipcc/info\\_for\\_analysts.php#time\\_info](http://www-pcmdi.llnl.gov/ipcc/info_for_analysts.php#time_info)) contains information about the experiments (and dates) from which the A1B integrations were initialized. In most but not all cases, the SRES A1B integrations were spawned from 20CEN simulations which are publicly available in the CMIP-3 archive. The notable exceptions are IPSL-CM4 and PCM. In cases where models were excluded from our analysis, or where the splicing of the 20CEN and A1B runs involved specific data processing choices, the justification for model exclusion (or the processing choices made) are detailed below.

**CNRM-CM3 model**

We did not include the CNRM-CM3 model in the analysis of spliced 20CEN/A1B runs. We took this decision because the CNRM group stored atmospheric temperature data at different vertical resolutions in the 20CEN and A1B integrations. This difference in vertical resolution introduces a discontinuity in the computed synthetic MSU temperatures at the splice point between the 20CEN and A1B runs (in December 1999). There is also a change in the number of vertical levels within the 20CEN run itself (between December 1899 and January 1900), which introduces another ‘jump’ in synthetic satellite temperatures.

**ECHAM5/MPI-OM**

As described in [http://www-pcmdi.llnl.gov/ipcc/info\\_for\\_analysts.php#time\\_info](http://www-pcmdi.llnl.gov/ipcc/info_for_analysts.php#time_info), the last available month of the ECHAM5/MPI-OM 20CEN experiment should be December 2000 (for all four of the ECHAM5/MPI-OM 20CEN realizations). However, MPI provided PCMDI with 20CEN data ending

in 2100, 2050, 2100, and 2000 (for runs1, 2, 3, and 4, respectively). The first available month of all four of the ECHAM5/MPI-OM A1B realizations is January 2001. To ensure correct splicing of data from the 20CEN and A1B experiments, we truncated runs1, 2, and 3 of the ECHAM5/MPI-OM 20CEN experiment after December 2000. Since run4 of the 20CEN experiment already ended in December 2000, it required no truncation.

### **GISS-ER**

For the GISS-ER model, run3 of the 20CEN experiment ends in December 2100, while run3 of the GISS-ER A1B experiment commences in January 2004. We dealt with this overlap of the historical and scenario experiments in the following way. According to [http://www-pcmdi.llnl.gov/ipcc/info\\_for\\_analysts.php#time\\_info](http://www-pcmdi.llnl.gov/ipcc/info_for_analysts.php#time_info), run3 of the 20CEN experiment should end in December 2003. The 97 years of post-2003 data in 20CEN run3 “should be identical to the data stored in the committed climate change experiment”. We therefore removed post-2003 data from 20CEN run3 before splicing the GISS-ER 20CEN data with A1B run3.

### **IPSL-CM4**

For the IPSL-CM4 model, the A1B run1 was initialized from the 20CEN run0. Because of a bug in the sulfate aerosol forcing in run0, this 20CEN realization was not provided to PCMDI (see [http://www-pcmdi.llnl.gov/ipcc/info\\_for\\_analysts.php#time\\_info](http://www-pcmdi.llnl.gov/ipcc/info_for_analysts.php#time_info)). Although the IPSL group notes that 20CEN run1 (which was provided to PCMDI, and which does not have a bug in the sulfate aerosol forcing) is similar to 20CEN run0 in the year 2000, we have not attempted to splice the IPSL-CM4 A1B run1 with run1 of the 20CEN simulation. In general, if the experiment from which the A1B run was initialized was not publicly available for a given model, we excluded that model from our analysis. This is why we did not produce spliced 20CEN/A1B data for the IPSL-CM4

model.

## PCM

The PCM A1B runs1, 2, 3, and 4 were not initialized from 20CEN experiments stored in the CMIP-3 archive. Instead, they were spawned from the January 1, 2000, conditions of PCM runs B06.08, B05.08, B06.05, and B06.27 (respectively). B06.08, B05.08, B06.05, and B06.27 involved estimated historical changes in anthropogenic factors only (well-mixed GHGs, sulfate aerosol direct effects, and tropospheric and stratospheric ozone). The official PCM 20CEN runs in the CMIP-3 archive have combined forcing by both anthropogenic and natural factors (changes in solar irradiance and volcanic aerosols).

The PCM runs B06.08, B05.08, B06.05, and B06.27 are publicly available from the National Center for Atmospheric Research. We were therefore able to calculate synthetic MSU temperatures from these simulations and splice them together with synthetic MSU temperatures from the PCM A1B runs1, 2, 3, and 4 (respectively). Although this processing step relies (at least in part) on PCM data which are not part of the official CMIP-3 archive, it can be independently replicated by other analysts.

Additional data processing steps performed with PCM data are listed below:

1. September 1870 was the first month of the PCM B06.08 run from which the A1B run1 was initiated. To avoid inclusion of incomplete years, data prior to January 1871 were truncated from B06.08 prior to splicing with A1B run1.
2. Data for November and December 2099 are missing from PCM A1B run1. To avoid including incomplete years, data were truncated after December 2098.
3. May 1960 was the first month of the PCM B05.08 run from which the A1B run2 was initiated. To avoid inclusion of incomplete years, data prior to January 1961 were truncated from B05.08



prior to splicing with A1B run2.

4. September 1871 was the first month of the PCM B06.05 run from which the A1B run3 was initiated. To avoid inclusion of incomplete years, data prior to January 1872 were truncated from B06.05 prior to splicing with A1B run3.
5. March 1870 was the first month of the PCM B06.27 run from which the A1B run4 was initiated. To avoid inclusion of incomplete years, data prior to January 1871 were truncated from B06.27 prior to splicing with A1B run4.

### **UKMO-HadCM3**

The UKMO-HadCM3 A1B run1 was spawned from run2 of the UKMO-HadCM3 20CEN simulation. In all other models, run1 of the A1B experiment was initiated from the end of run1 of the 20CEN simulation. Note that run 1 of the UKMO-HadCM3 A1B experiment has missing data in March 2106. Synthetic MSU temperatures could not be computed for this month. To guard against erroneous use of March 2106 in analyses of synthetic MSU data, we truncated the A1B results for UKMO-HadCM3 in December 2105 (*i.e.*, at the end of the last complete year before the missing month).

### **UKMO-HadGEM1**

The last year of run1 of the UKMO-HadGEM1 A1B experiment ends in November 2199. To avoid the inclusion of incomplete years, A1B data were truncated after December 2198.

Table S3: Basic information relating to CMIP-3 pre-industrial control integrations.

	Model	Realization	First year	Last year	No. of months
1	BCCR-BCM2.0	run1	1850	2099	3000
2	CCCma-CGCM3.1(T47)	run1	1850	2850	12012
3	CCCma-CGCM3.1(T63)	run1	1850	2199	4200
4	CCSM3	run1	280	509	2760
5	CCSM3	run2	300	799	6000
6	CNRM-CM3	run1	1930	2429	6000
7	CSIRO-Mk3.5	run1	1871	2200	3960
8	CSIRO-Mk3.5	run2	2401	2870	5640
9	ECHAM5/MPI-OM	run1	2150	2655	6072
10	GFDL-CM2.0	run1	1	500	6000
11	GFDL-CM2.1	run1	1	500	6000
12	GISS-AOM	run1	1850	2100	3012
13	GISS-AOM	run2	1850	2100	3012
14	GISS-EH	run1	1880	2279	4800
15	GISS-ER	run1	1901	2400	6000
16	FGOALS-g1.0	run1	1850	2199	4200
17	INGV-SXG	run1	1761	1860	1200
18	INM-CM3.0	run1	1871	2200	3960
19	IPSL-CM4	run1	1860	2359	6000
20	MIROC3.2(hires)	run1	1	100	1200
21	MIROC3.2(medres)	run1	2300	2799	6000
22	MRI-CGCM2.3.2	run1	1851	2200	4200
23	PCM	run1	100	449	4200
24	PCM	run2	451	739	3468
25	PCM	run3	750	1049	3600
26	UKMO-HadCM3	run1	1859	2199	4092
27	UKMO-HadCM3	run2	1859	1939	972
28	UKMO-HadGEM1	run1	1860	1925	792
29	UKMO-HadGEM1	run2	1860	1927	2098

**Table S3: Processing notes for CMIP-3 pre-industrial control runs****CSIRO-Mk3.5**

In the CSIRO-Mk3.5 pre-industrial control run data, there is a gap in the time axis of the atmospheric temperature data. Data are missing from January 2201 to December 2400. This introduces a gap in the synthetic MSU temperature data. To deal with this problem, synthetic MSU temperature data from the CSIRO-Mk3.5 pre-industrial control run were split into two segments. The first segment of the data extends from January 1871 to December 2200. The second segment of the data is from January 2401 to December 2870. In our analysis, segments 1 and 2 are given the designations run1 and run2.

**FGOALS-g1.0**

The FGOALS-g1.0 model has three (supposedly independent) realizations of the pre-industrial control run (referred to as run1, run2, and run3). These three realizations are not independent: run2 and run3 are time-shifted duplicates of run1. The time shift appears to be by six years. To guard against the possibility that users might regard each of these ensemble members as an independent realization of natural internal variability, we provide synthetic MSU temperatures for run1 only.

**ECHAM5/MPI-OM**

Synthetic MSU temperatures from the ECHAM5/MPI-OM pre-industrial control run were originally calculated using erroneous atmospheric temperature and surface pressure data. The erroneous data spanned the period 1786 to 2117. The metadata (in the “title” information of the NetCDF file) incorrectly identified the ECHAM5/MPI-OM pre-industrial control run as a 20CEN run. Additionally, the time axis was incorrect. These erroneous ECHAM5/MPI-OM data were later replaced. The new

pre-industrial control run data incorporated the correct title and time axis, and spanned the period 2150 to 2655. After a PCMDI server crash, both the (older) incorrect atmospheric temperature and surface pressure data and the (newer) corrected data were retrieved. To avoid the possibility that other analysts might use erroneous ECHAM5/MPI-OM data in the calculation of synthetic MSU temperatures, all of the older, incorrect data files were removed. Our synthetic MSU temperatures for the ECHAM5/MPI-OM pre-industrial control run were calculated using the newer, correct data.

### **PCM**

In the PCM atmospheric temperature, surface temperature, and surface pressure data, there are two separate “jumps” in the time axis. The first discontinuity is between December of year 449 and November of year 450 (inclusive). The second discontinuity is between December of year 739 and January of year 750. To deal with these discontinuities, the PCM pre-industrial control run was split into three segments. Each segment contains complete years only. Segment 1 extends from January of year 100 to December of year 449. Segment 2 extends from January of year 451 to December of year 739. Segment 3 spans the period January of year 750 to December of year 1049. Segments 1, 2, and 3 are given the designations run1, run2, and run3 (respectively).

### **UKMO-HadCM3**

In run1 of the UKMO-HadCM3 pre-industrial control, the surface temperature data are 12 months longer than the datasets used for other datasets used for calculating synthetic MSU temperatures. To minimize the possibility of errors arising from such differences in record length, surface temperature data for the final year (2200) of run1 were removed.

**UKMO-HadGEM1**

The UKMO-HadGEM1 pre-industrial control run has two months with missing atmospheric temperature, surface temperature, and surface pressure data (June 1926 and April 2099). To exclude these missing months, the control run was split into two segments. Each segment contains complete years only. Segment 1 extends from January 1860 to December 1925 (inclusive). Segment 2 spans the period January 1927 to December 2098. Segments 1 and 2 are given the designations run1 and run2 (respectively). Note also that the first month of the UKMO-HadGEM1 pre-industrial control run is a December. In all other model pre-industrial control runs, the first month is a January. To guard against processing errors, the initial December was removed from all synthetic MSU temperatures calculated with UKMO-HadGEM1 pre-industrial control run data.

## Captions for Figures in Supporting Text

**Figure S1:** Sensitivity of estimated  $\overline{p}_f'$  values to trend fitting method. The results for least-squares linear trends are the same as those shown and described in Figure 6E. The  $\overline{p}_f'$  values for an alternative linear trend estimator, the least absolute deviation [LAD; see *Press et al.*, 1992] were calculated with exactly the same model and observational TLT data used in the least-squares approach. All aspects of the  $\overline{p}_f'$  value calculation are identical in the least-squares and LAD cases.

**Figure S2:** Response functions for Butterworth band-pass and high-pass filters. The band-pass filter focuses on variability on timescales of 10 years, with half-power points at 5 and 20 years, while the high-pass filter has a half-power point at two years, and excludes all variability on timescales longer than 5 years.

# Sensitivity of Weighted $\bar{p}_f$ Values to Trend-Fitting Method

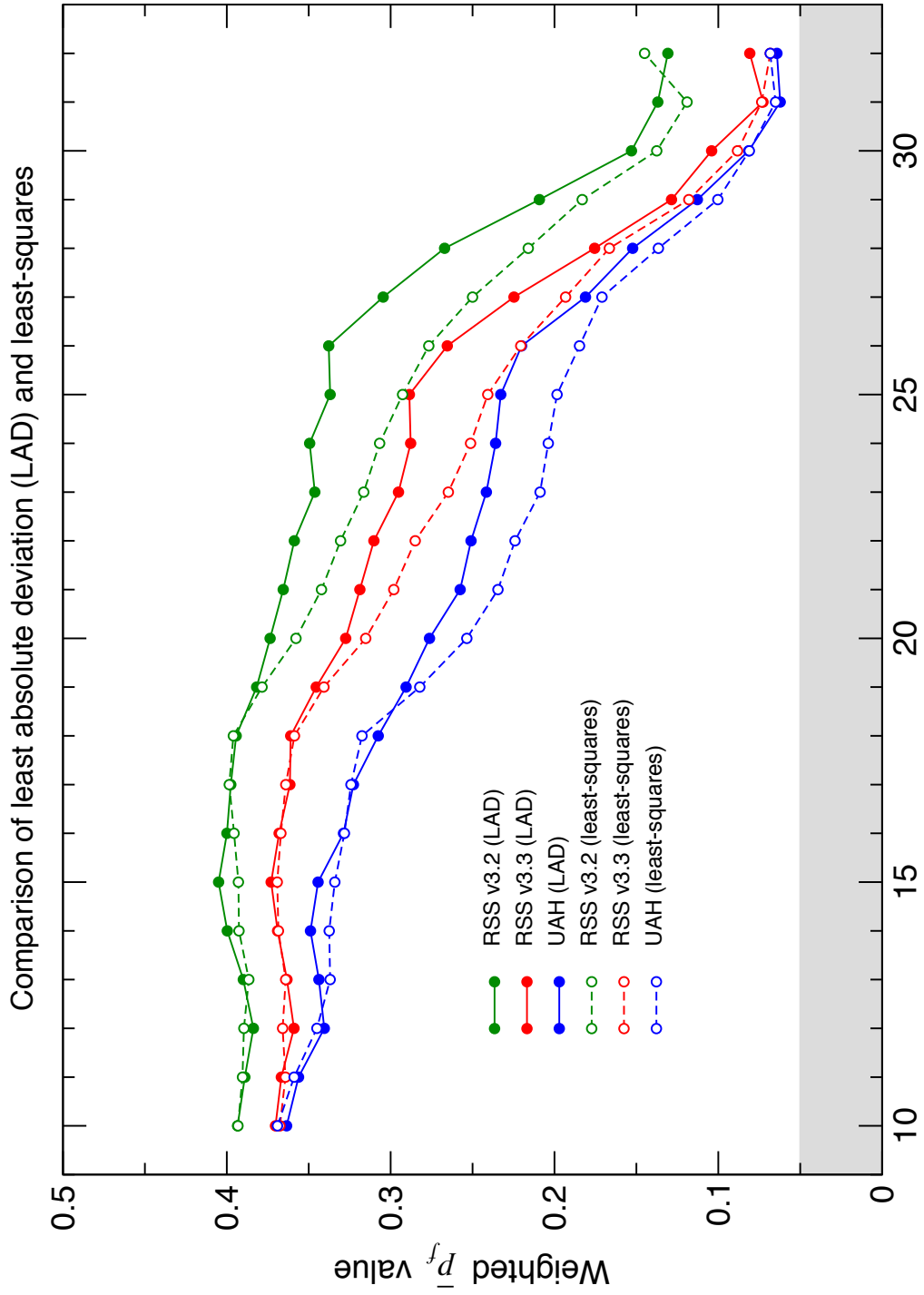


Figure S1: Santer et al.

Response Functions for Butterworth Band-pass and High-pass Filters

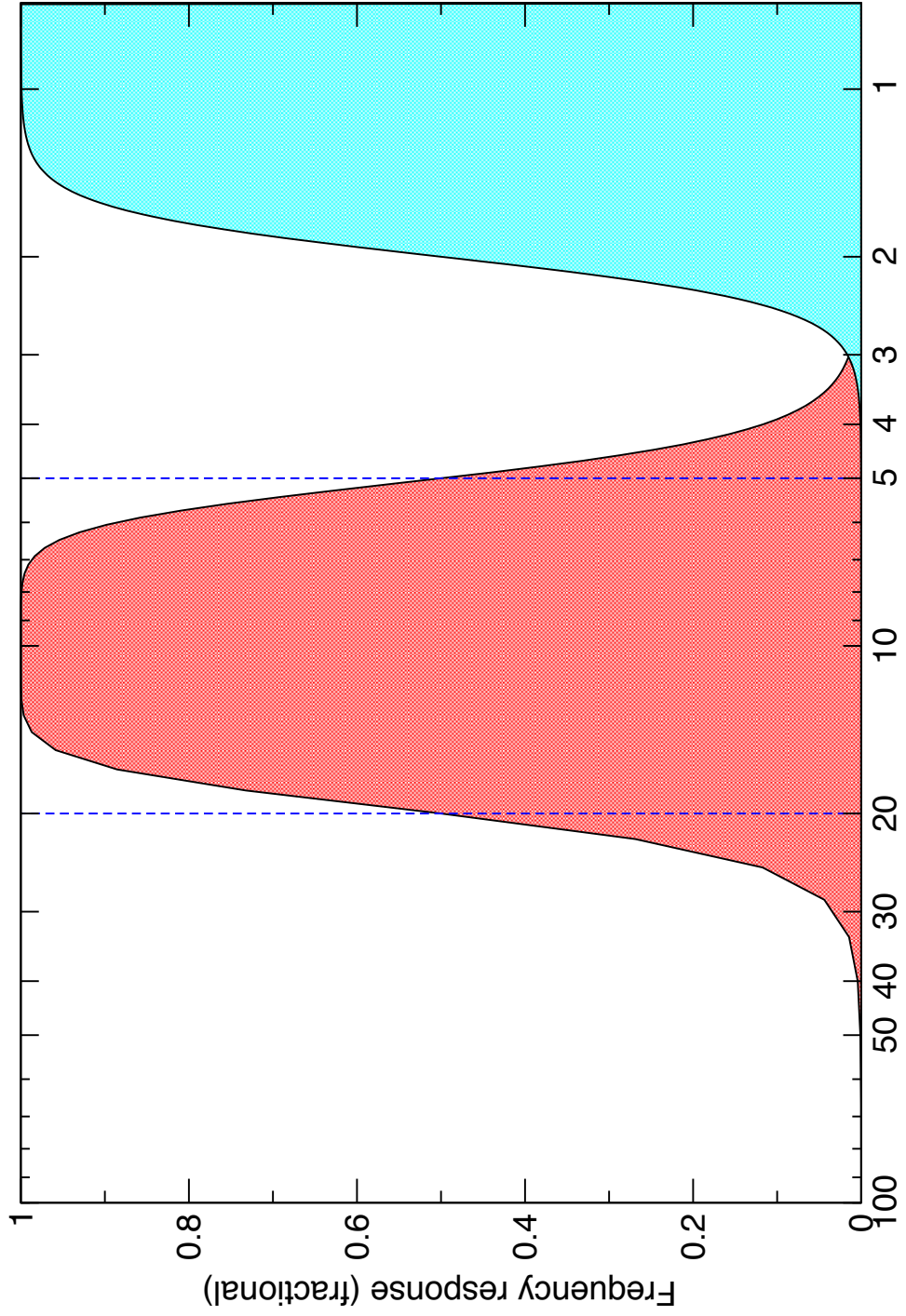


Figure S2: Santer et al.